

## ***Project 55: Fe-Containing Multi-Principal Element Alloys for Protective Structures***

***Semi-annual Fall Meeting  
October 2021***



- Student: James Frishkoff (Mines)
- Faculty: Dr. Amy Clarke & Dr. Kester Clarke (Mines)
- Industrial Mentors: Bruce Antolovich (ATI), Hayley Brown (SFSA), *Steve Jansto (CBMM), Tanya Ros (Arcelor Mittal)*

# Project 55: Fe-Containing Multi-Principal Element Alloys for Protective Structures



- Student: James Frishkoff (Mines)
- Advisors: Amy Clarke, Kester Clarke (Mines)

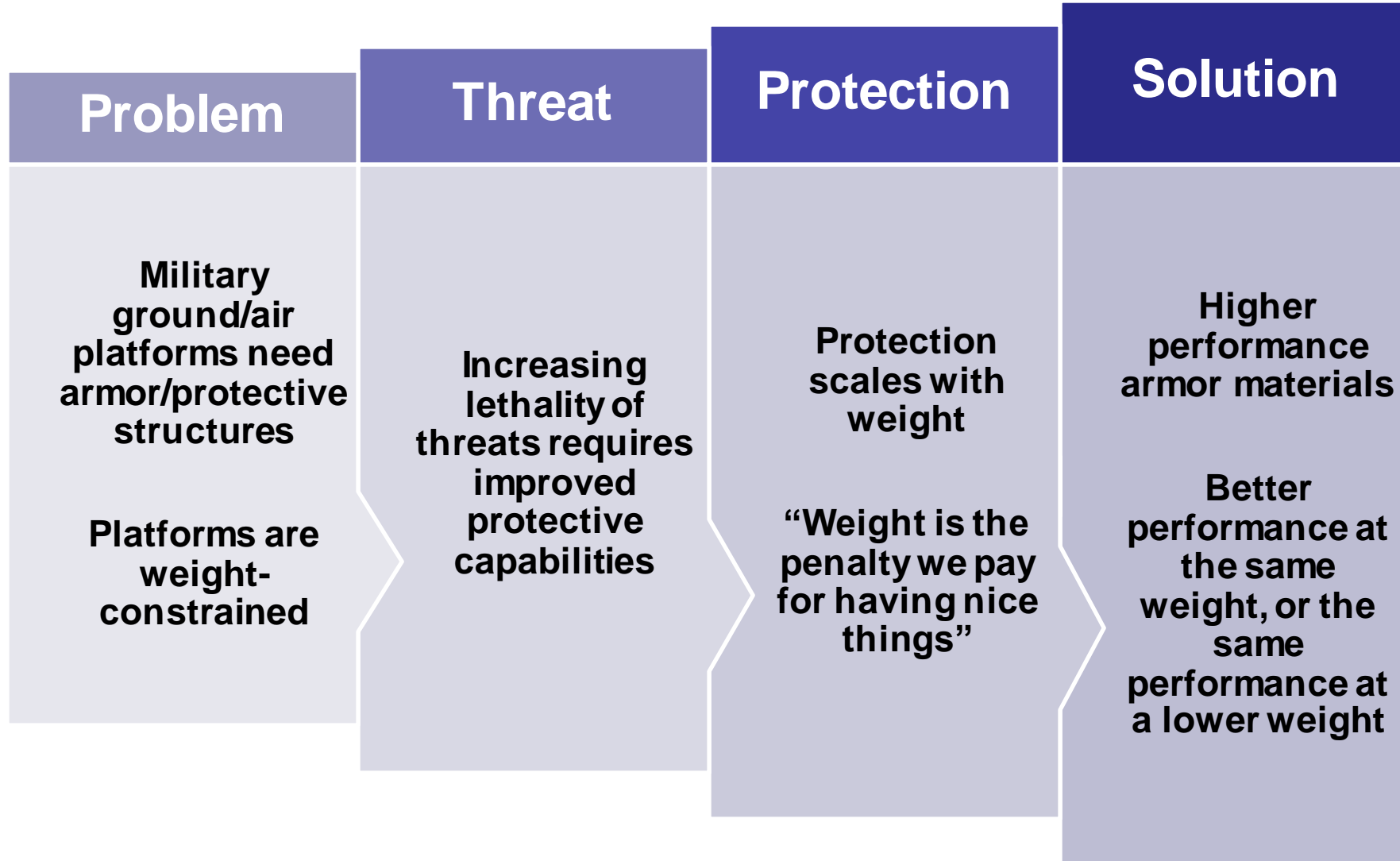
**Project Duration**  
MS: January 2021 to December 2022

- **Problem:** TRIP/TWIP MPEAs currently rely on costly high alloy content, and composition dependence not yet well understood.
- **Objective:** Achieve TRIP/TWIP & strength-ductility combinations in Co-lean MPEAs via experimental methods and high-throughput thermodynamic modeling.
- **Benefit:** Increasingly high strength-ductility combinations desired in many sectors, including vehicle protective structures.

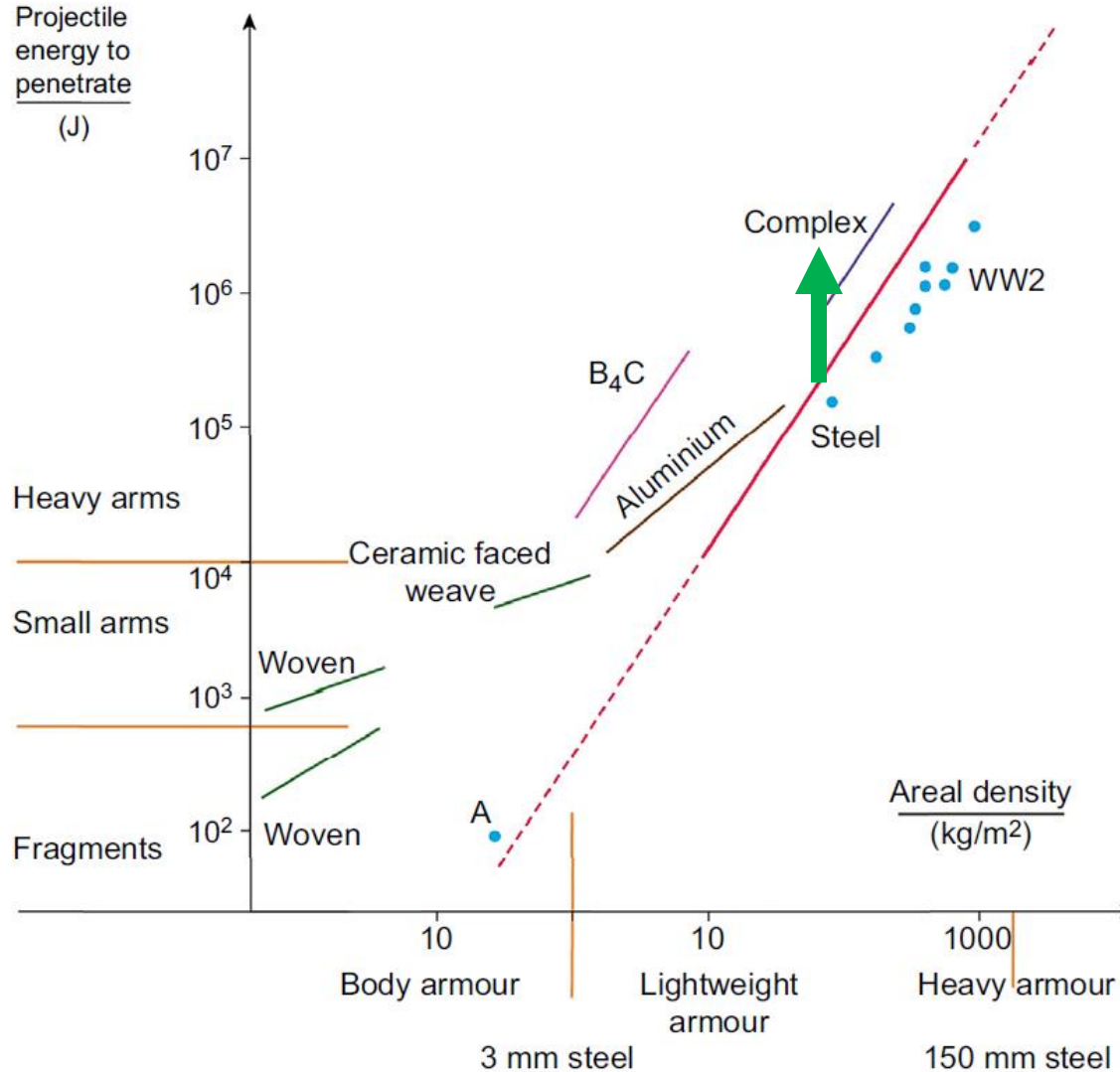
- Recent Progress**
- Multi-factor computer-aided alloy design initiated and seven promising alloy candidates identified
  - Microstructural evaluation of existing CoCrNi TRIP-MPEA family initiated
  - Three baseline alloys sourced from ATI for comparison
  - New arc melting furnace being installed – rapid small batch melting

Metrics		
Description	% Complete	Status
1. Literature review	40%	●
2. ThermoCalc, PanDat & LAMMPS modeling	60%	●
3. Obtain industrial baseline material	100%	●
4. Alloy downselect	15%	●
5. Gleeble experiments on downselected alloys and industrial reference material	5%	●

# The Problem Space



# The Problem Space – Protective Structure Performance Metrics

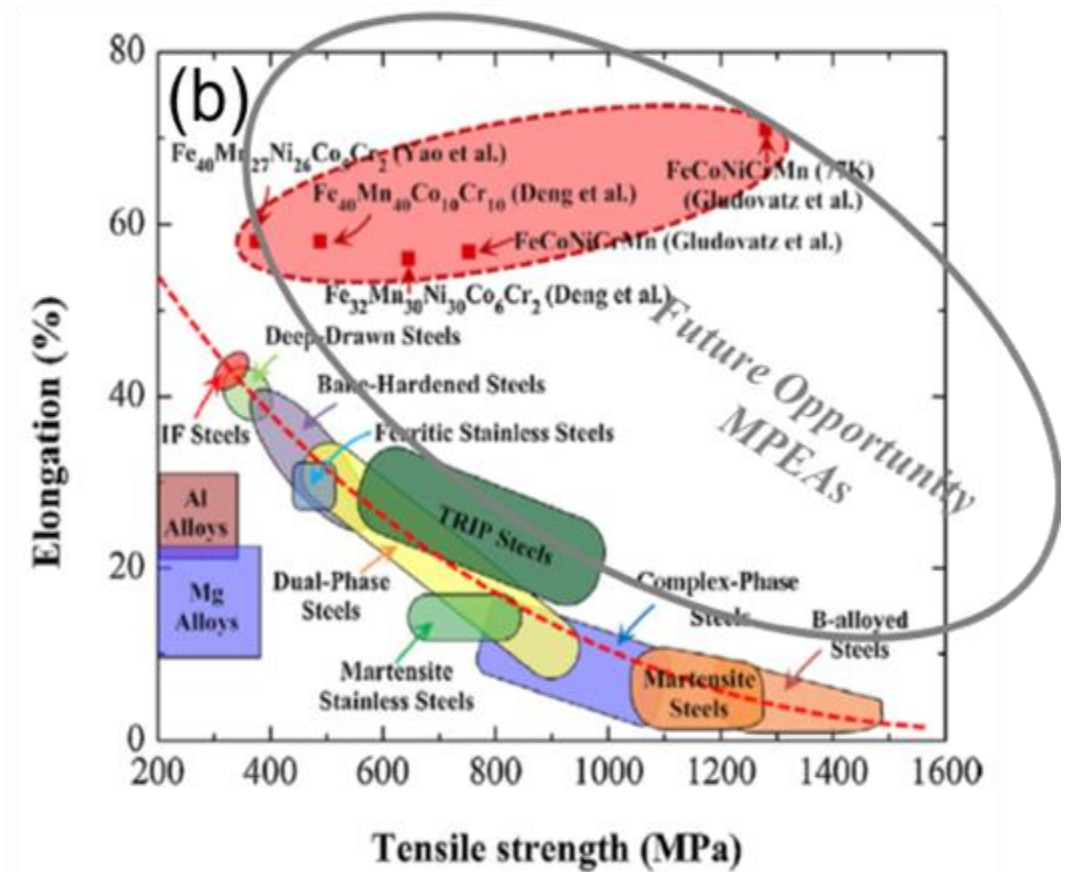
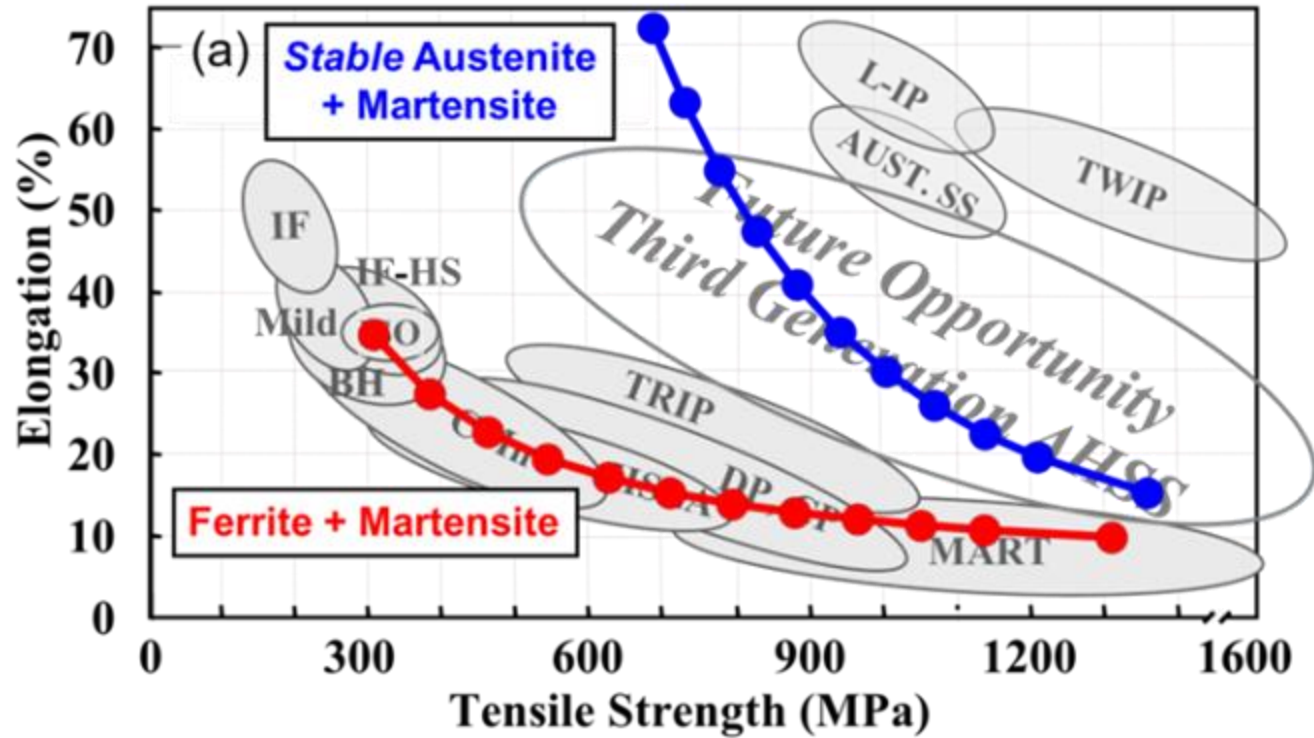


Wants and needs:

- Yield & Dynamic Flow Stress (quasistatic up to  $10^4 \text{ s}^{-1}$ )
- Ultimate Tensile Strength
- Strain to Fracture
- Work Hardening Rate
- Shear Strain Localization Resistance
- Surface Hardness
- Weldability

I. Crouch, *The Science of Armour Materials*, Elsevier (2017). Reproduced from A. Doig, *Military Metallurgy*, Maney Publishing: London (1998)

# Steel Example: Austenite/Martensite Mixtures Create Desirable Property Combinations



D.K. Matlock and J.G. Speer, "Design considerations for the next generation of advanced high strength steels", In Proceedings of The 3<sup>rd</sup> International Conference on Advanced Structural Steels, Gyeongju, Korea, 2006, pp. 774-781

Y.F. Ye, Q. Wang, J. Lu, C.T. Liu, Y. Yang. "High-entropy alloy: challenges and prospects", Materials Today, 2011, 19(6):349-362

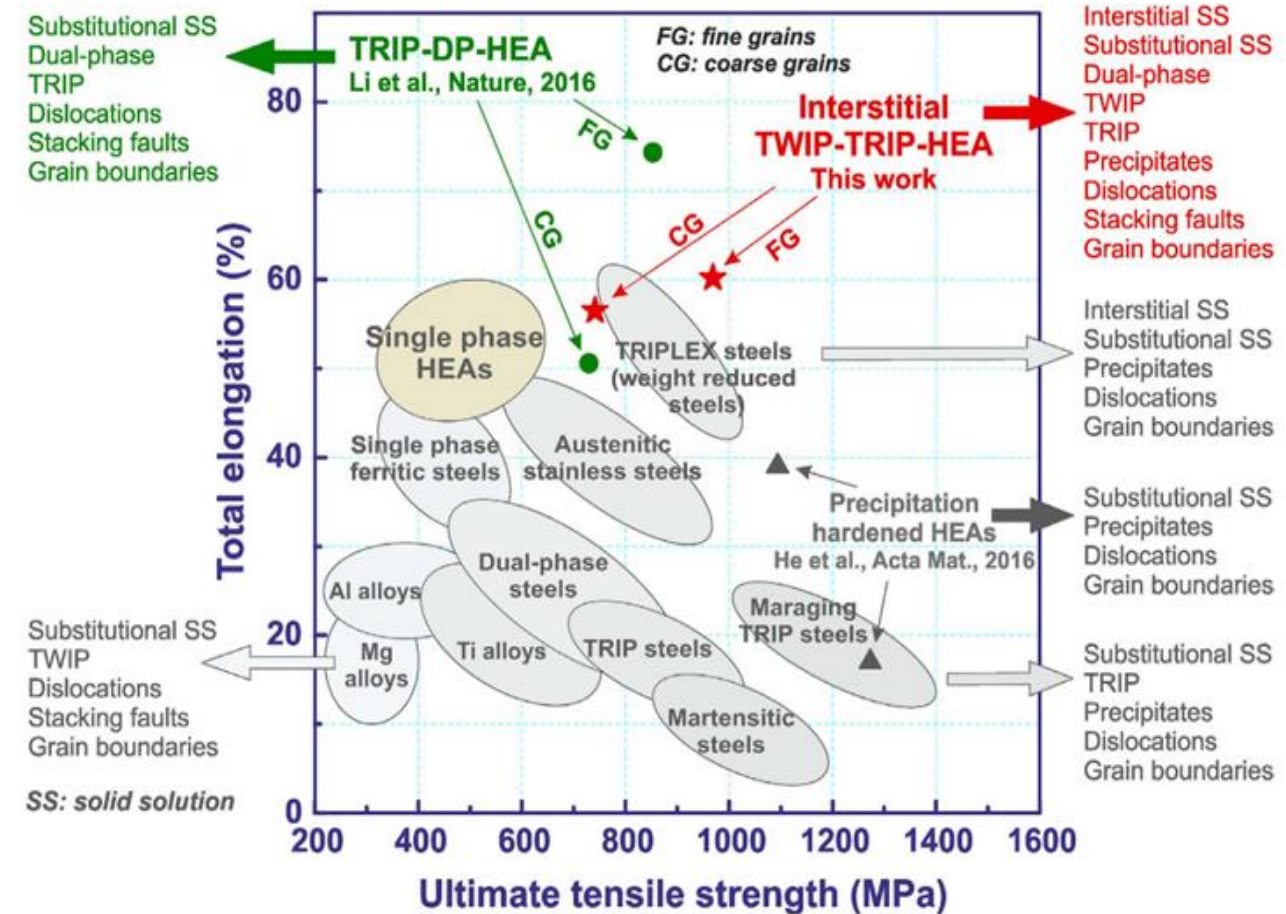
# Alloy Design Concepts

## Basic factors:

- Metastability (TRIP)
- Deformation twinning (TWIP)
- Solid solution strengthening
- Precipitation hardening
- Grain size

## Microstructural features:

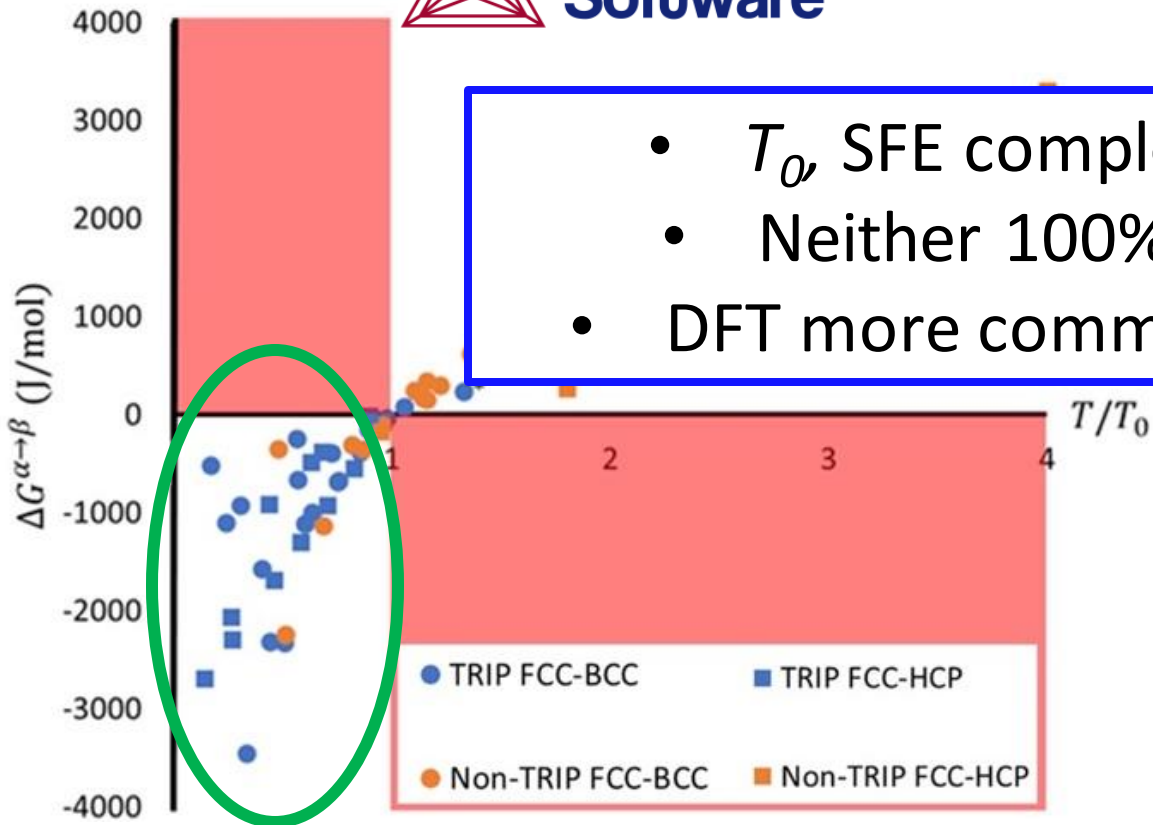
- Limit brittle IMs e.g sigma phase
- $\gamma'$  precipitate strengthening
- Other precipitates (carbides,  $\text{Fe}_2\text{SiTi}$ )
- GB pinning – precipitates, Nb
- Overaged precipitates (reduce ASB)



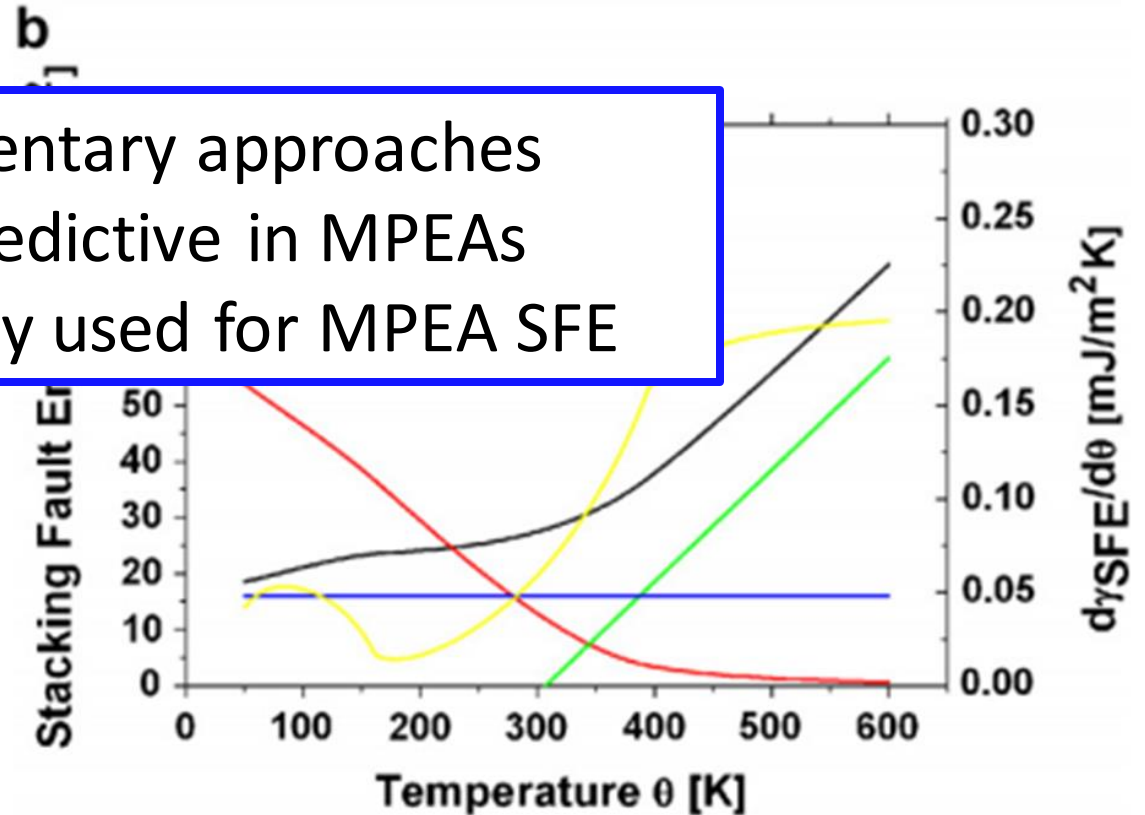
Z. Li et al, "Interstitial atoms enable joint twinning and transformation induced plasticity in strong and ductile high-entropy alloys", *Sci Rep*, 2017, 7:40704

# Computer-Aided Alloy Design – Metastability

 **Thermo-Calc  
Software**



- $T_0$ , SFE complementary approaches
- Neither 100% predictive in MPEAs
- DFT more commonly used for MPEA SFE

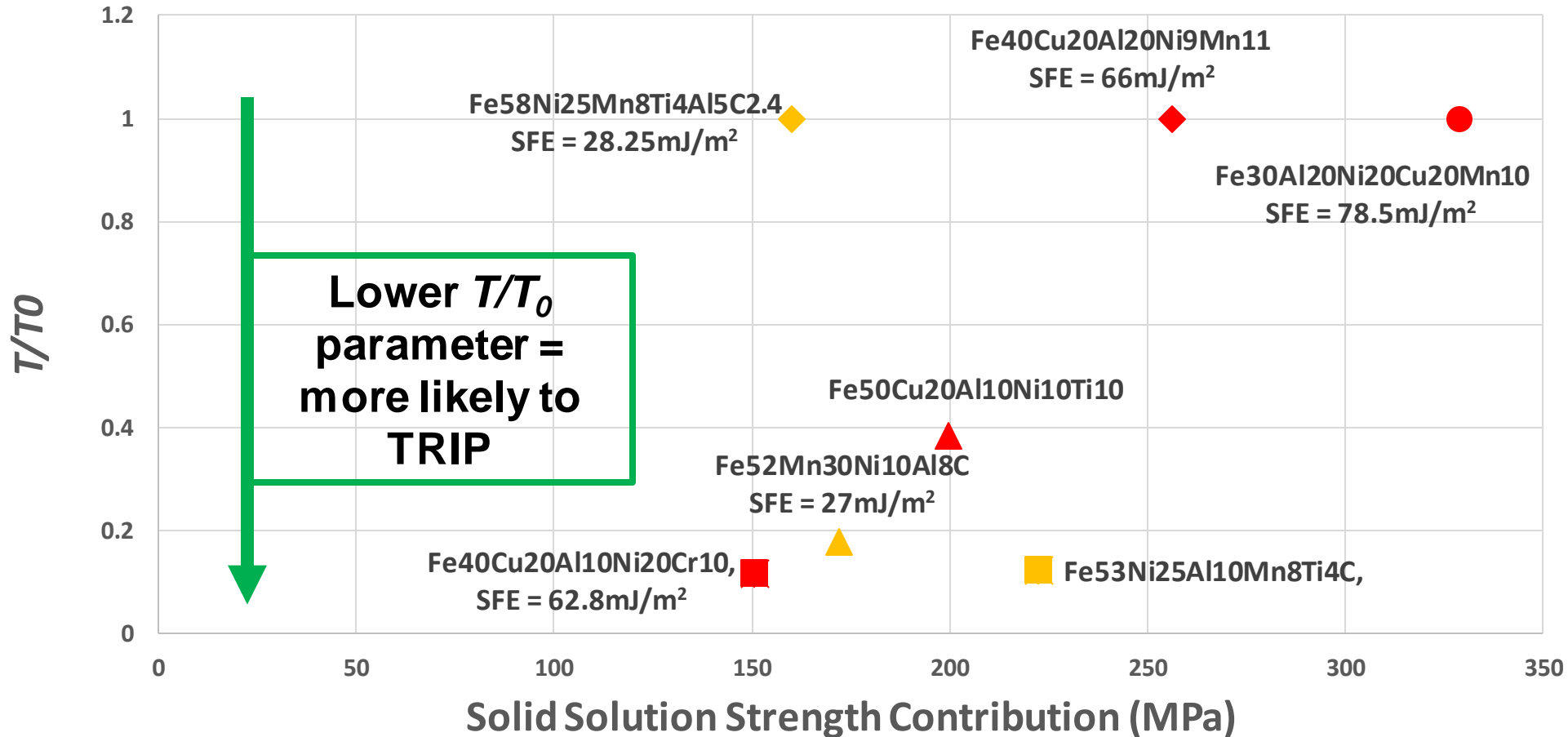


J.A. Copley, Prediction and Observation of Transformation-Induced Plasticity Behavior in CoCrNi Multi-Principal Element Alloys with In-Situ Synchrotron X-Ray Diffraction, MS Thesis, Colorado School of Mines, 2020

Curtze, S., and V. T. Kuokkala. "Dependence of Tensile Deformation Behavior of TWIP Steels on Stacking Fault Energy, Temperature and Strain Rate." *Acta Materialia* 58, no. 15 (September 1, 2010): 5129–41. <https://doi.org/10.1016/J.ACTAMAT.2010.05.049>.

# Computer-Aided Alloy Design – Metastability

## Solid Solution Strengthening & Metastability



Solid solution strengthening calculated via TC-EARS method, Coury et al, *Sci Reps* June 2018  
(<https://doi.org/10.1038/s41598-018-26830-6>)

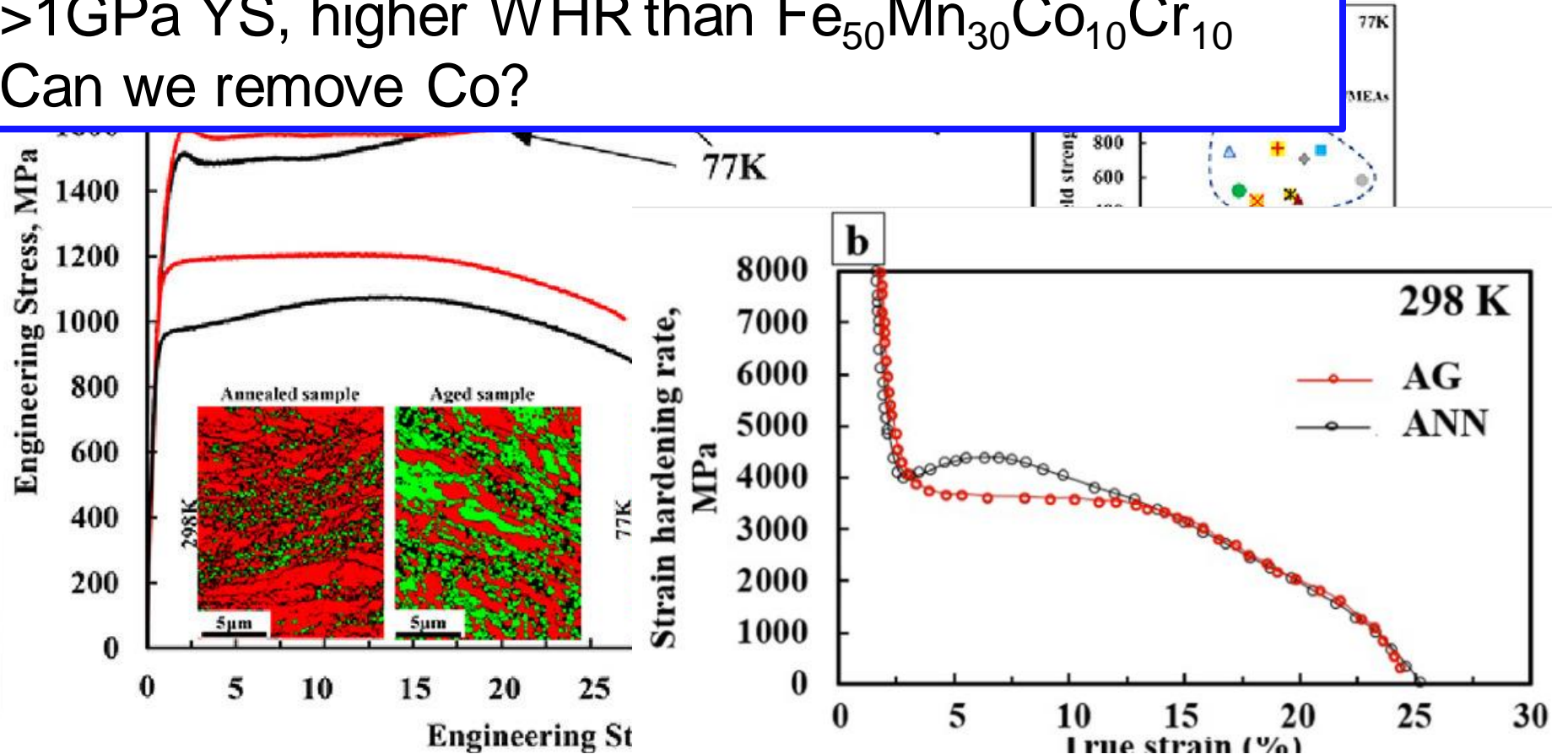
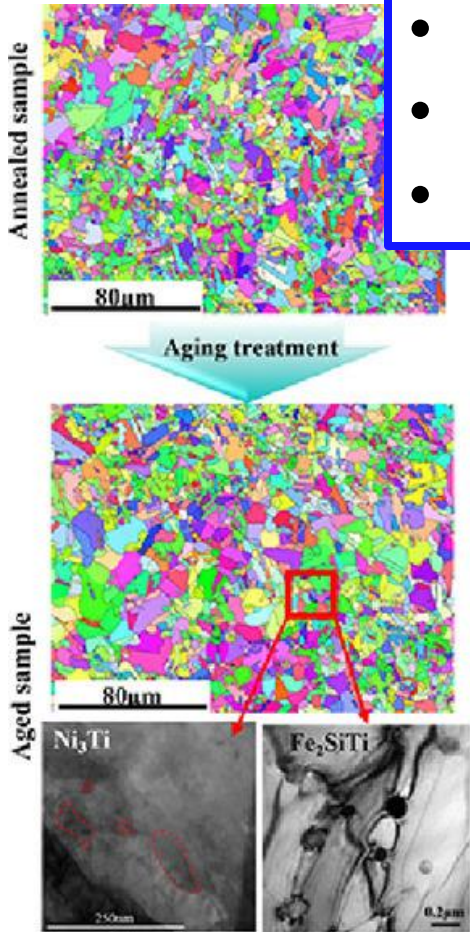
All SFE values calculated via modified Olson-Cohen method of Curtze et al., *Acta* Feb. 2011  
([doi.org/10.1016/j.actamat.2010.10.037](https://doi.org/10.1016/j.actamat.2010.10.037))



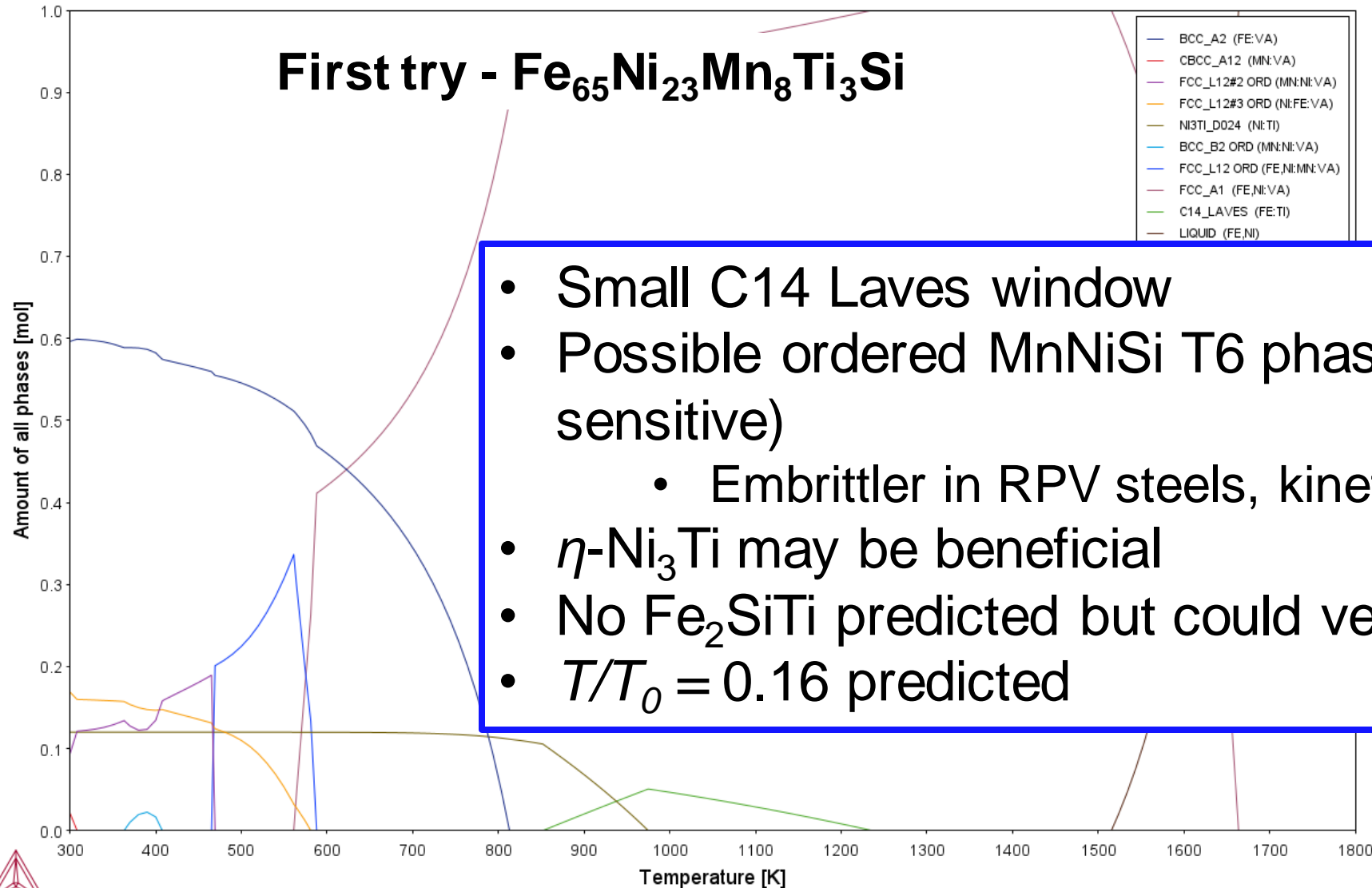
# New Developments in Literature

## $Fe_{65}Ni_{15}Co_8Mn_8Ti_3Si$ – Nene et al. 2021

- TRIP/TWIP active with fine precipitates
- >1GPa YS, higher WHR than  $Fe_{50}Mn_{30}Co_{10}Cr_{10}$
- Can we remove Co?



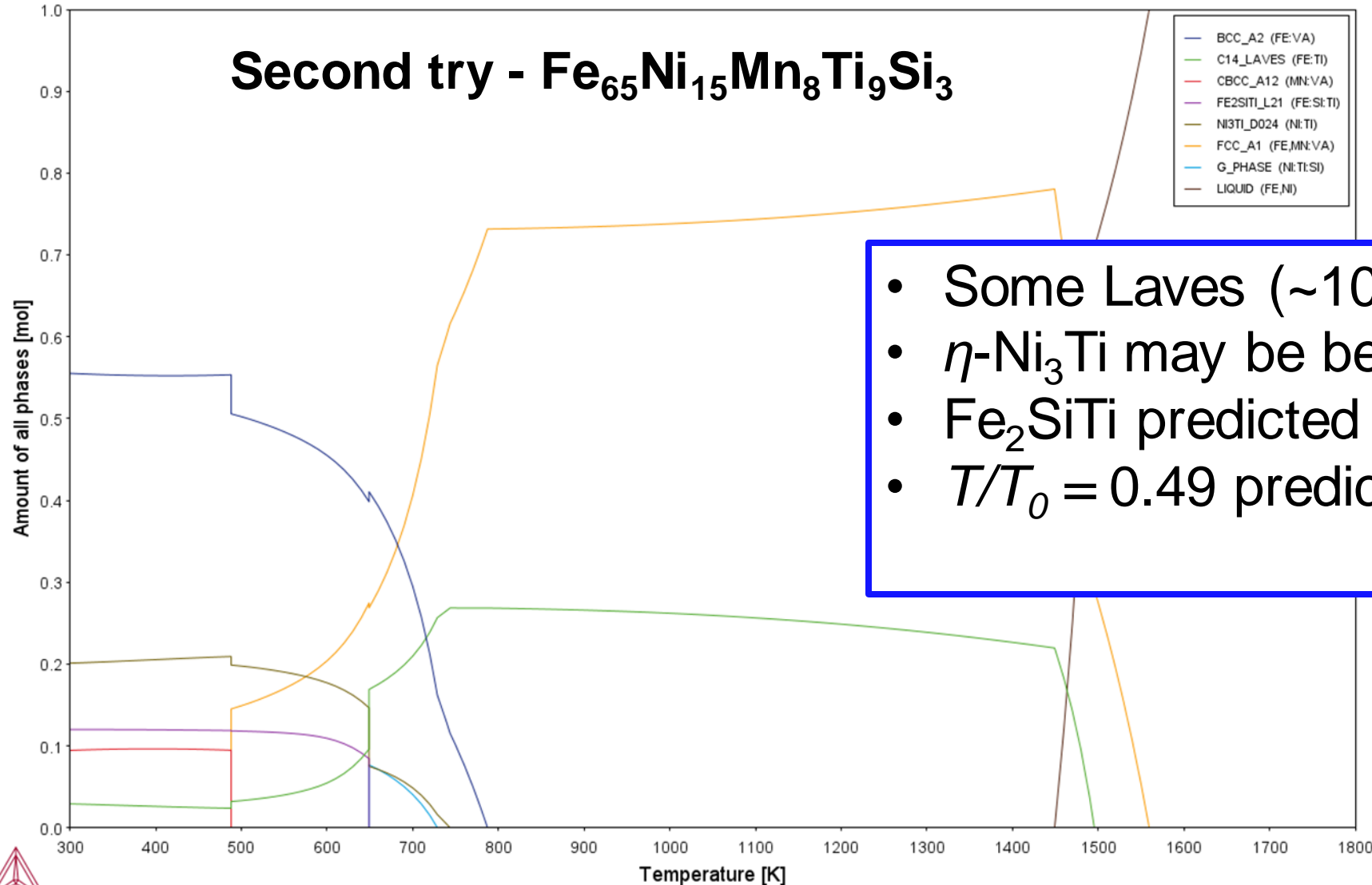
# New Developments in Literature



- Small C14 Laves window
- Possible ordered MnNiSi T6 phase (database sensitive)
  - Embrittler in RPV steels, kinetics unknown
- $\eta$ -Ni<sub>3</sub>Ti may be beneficial
- No Fe<sub>2</sub>SiTi predicted but could verify experimentally
- $T/T_0 = 0.16$  predicted



# New Developments in Literature

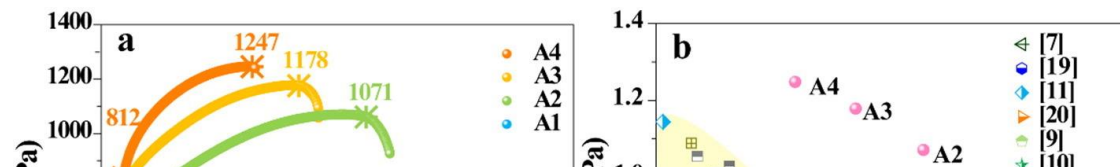


- Some Laves (~10% <350°C)
- $\eta$ -Ni<sub>3</sub>Ti may be beneficial
- Fe<sub>2</sub>SiTi predicted (12%)
- $T/T_0 = 0.49$  predicted

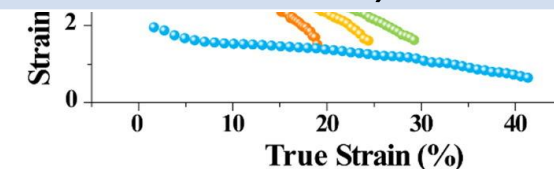
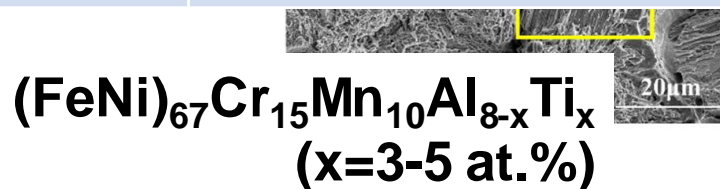


# Computer-Aided Alloy Design – $\gamma/\gamma'$ Strengthening

- $\gamma'$  strengthened TRIP-assisted armor steel (Wengrenovich 2016)

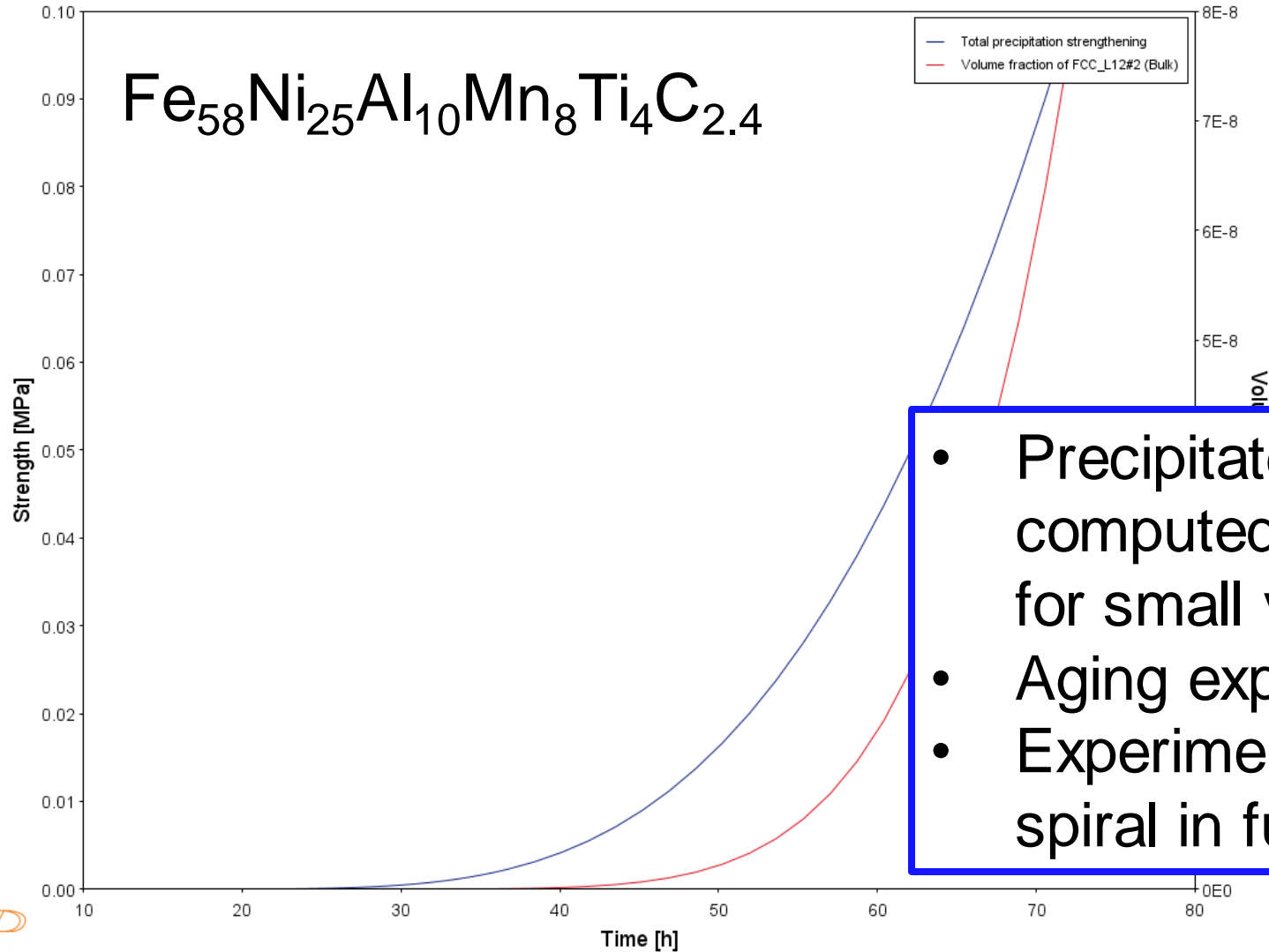


Composition	Max $\gamma'$ %	Sigma phase	Other Precipitates
$\text{Fe}_{58}\text{Ni}_{25}\text{Al}_{10}\text{Mn}_8\text{Ti}_4\text{C}_{2.4}$	15% - 330°C	None	$\eta\text{-Ni}_3\text{Ti}$ (5%)
$\text{Fe}_{45}\text{Ni}_{28}\text{Cr}_8\text{Mn}_8\text{Al}_5\text{Ti}_6\text{Nb}_{.25}$	28% - 225°C	Present @ all $\gamma'$ T, ~20%	$\eta\text{-Ni}_3\text{Ti}$ (26% @ 500°C)
$(\text{FeNi})_{67}\text{Cr}_{15}\text{Mn}_{10}\text{Al}_3\text{Ti}_5\text{Nb}_{.25}$	32% - 350°C	Present @ all $\gamma'$ T, ~35%	$\eta\text{-Ni}_3\text{Ti}$ (26% @ 550°C)



Zhao, Y. L. et al. Development of high-strength Co-free high-entropy alloys hardened by nanosized precipitates. *Scr. Mater.* 148, 51–55 (2018).

# Computer-Aided Alloy Design – $\gamma/\gamma'$ Strengthening



- Precipitate/age hardening MPEAS: computed kinetics slow (100s of hours for small vol.%)
- Aging experiments needed
- Experimental data  $\rightarrow$  positive feedback spiral in future modeling efforts



## Johnson-Cook

- Empirical
- Many modifications, but all have  $T$ , strain rate params
- Common in high rate & ballistics studies

$$\sigma_{\text{eq}} = [A + Bp^n] [1 + \dot{p}^*]^C [1 - T^{*m}]$$

## Zerilli-Armstrong

- Dislocation theory based
- Variants for crystal structure
- Also frequently modified, common in ballistics

$$\sigma_{\text{eq}} = \sigma_a + B \exp(-\beta T) + A \varepsilon_{\text{eq}}^n$$

↑ **BCC**      ↓ **FCC**

$$\sigma_{\text{eq}} = \sigma_a + A \varepsilon_{\text{eq}}^n \exp(-\alpha T)$$

Borvik, T., O. S. Hopperstad, T. Berstad, and M. Langseth. "A Computational Model of Viscoplasticity and Ductile Damage for Impact and Penetration." *European Journal of Mechanics - A/Solids* 20, no. 5 (September 1, 2001): 685–712. [https://doi.org/10.1016/S0997-7538\(01\)01157-3](https://doi.org/10.1016/S0997-7538(01)01157-3).

Dey, S., T. Børvik, O. S. Hopperstad, and M. Langseth. "On the Influence of Constitutive Relation in Projectile Impact of Steel Plates." *International Journal of Impact Engineering* 34, no. 3 (March 1, 2007): 464–86. <https://doi.org/10.1016/J.IJIMPENG.2005.10.003>.

# Mechanical Test Plan


T (°C)	Room Temperature	Temperature
Strain rate (s <sup>-1</sup> )		
Quasistatic (10 <sup>-3</sup> )	Tensile	
High (~100) -- Mid -- Low (10 <sup>-2</sup> )	Tensile	
	Tensile	
	Tensile	

ASTM E8 tensile      Gleeble Tensile

- 3 samples/condition
- More conditions = better constitutive model fitting
- Example T,  $\dot{\epsilon}$  from literature: 400 – 1000°C, 10<sup>-2</sup> – 10<sup>2</sup>/s (Saxena et al., *J Mater Eng Perf*, Sept 2019)

# Mechanical Test Plan

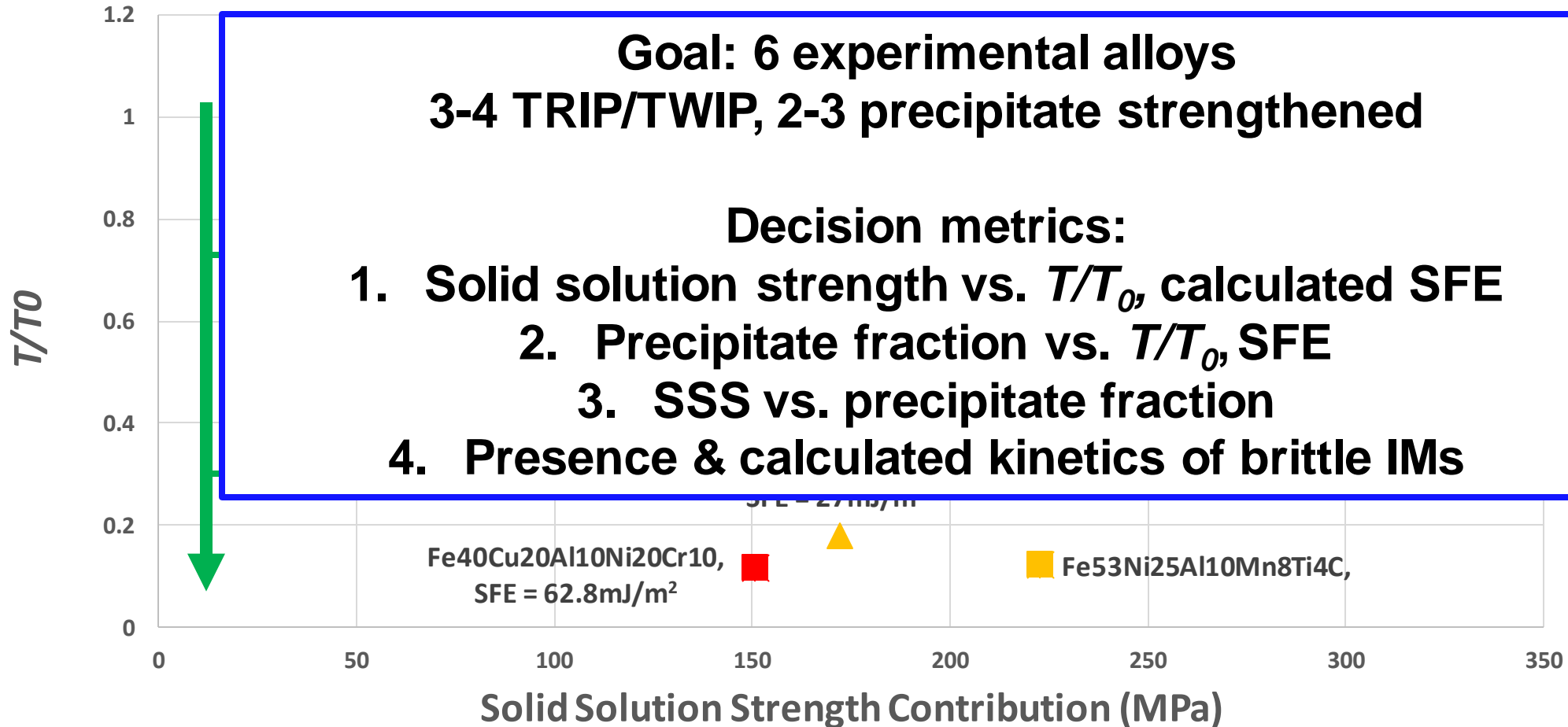
T (°C)	Room Temp	Warm Work Temperature	Hot Work/Supersolvus
Strain rate (s <sup>-1</sup> )			
Quasistatic (10 <sup>-3</sup> )	Gleeble Compression	Gleeble Compression	Gleeble Compression
High (~100) -- Mid -- Low (10 <sup>-2</sup> ) 	Gleeble Compression	Gleeble Compression	Gleeble Compression
		Gleeble Compression	Gleeble Compression

- 3 samples/condition
- Baseline processing data vs. conventional alloys
- Support future microstructural optimization work



# Downselect Progress

## Solid Solution Strengthening & Metastability



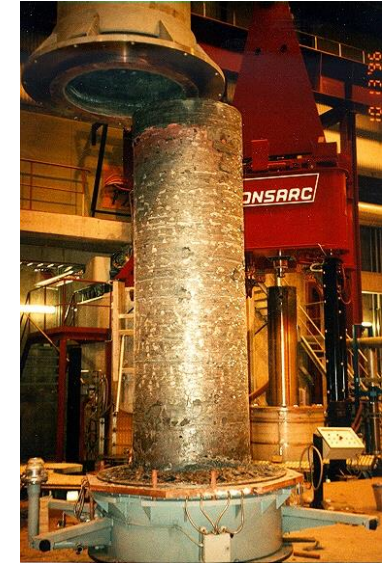
# Industry Partner – ATI Specialty Materials

## Added Capability

- 25 & 50 lb. vacuum melted ingots
- VAR/ESR for cleanliness
- Industrial thermomechanical processing & heat treatment

## Baseline Alloys

- ATI 188 – Co-base high-temp austenitic alloy; high work-hardening; TRIP?
- A286 – Legacy NiCr high-temp austenitic steel; TRIP?
- Datalloy HP – Highly alloyed steel; quasi-MPEA



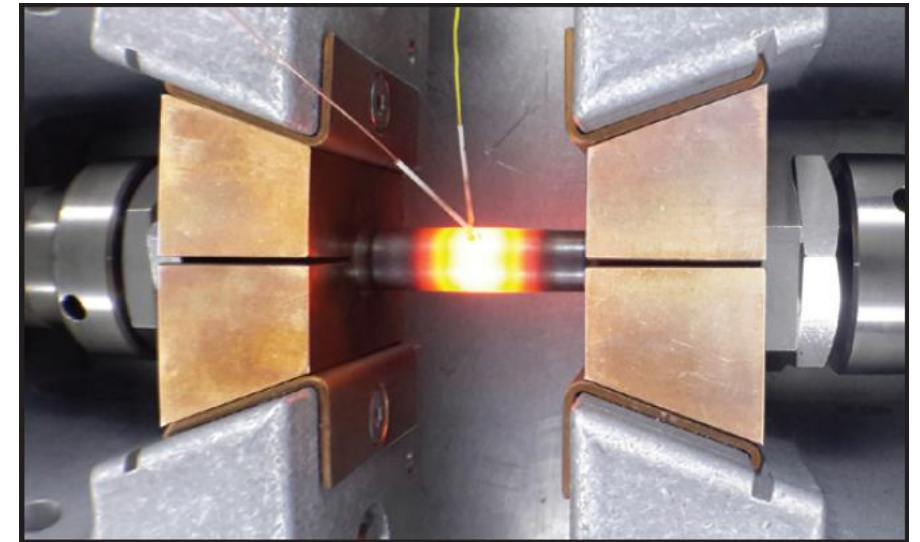
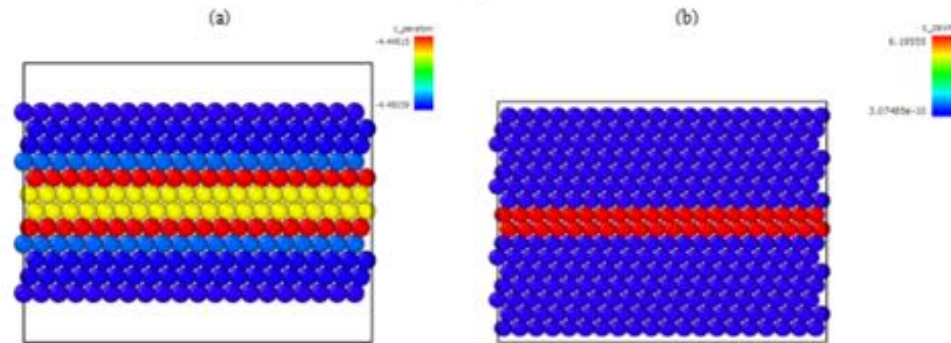
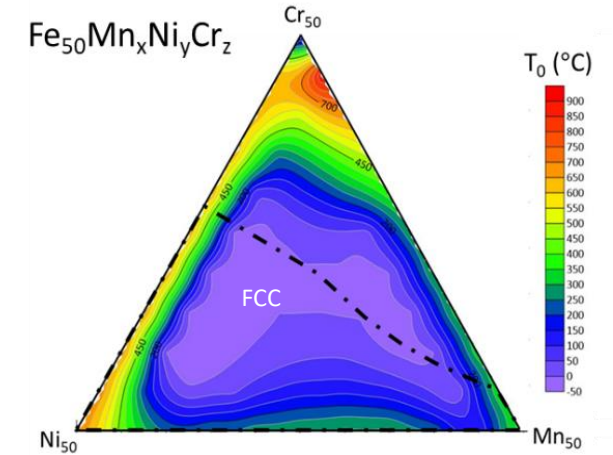
Composition Range (UNS N08830)			
Element	Wt. %	Element	Wt. %
Carbon	0.015	Manganese	3.0 – 6.0
Phosphorous	0.035	Sulfur	0.010
Silicon	1.00	Nickel	29.0 – 34.0
Chromium	20.0 – 24.0	Molybdenum	4.5 – 6.5
Copper	0.50 – 2.00	Cobalt	0.50 – 3.50
Tungsten	0.20 – 1.80	Nitrogen	0.20 – 0.55
Iron	balance		

Maximum % unless a range is indicated.

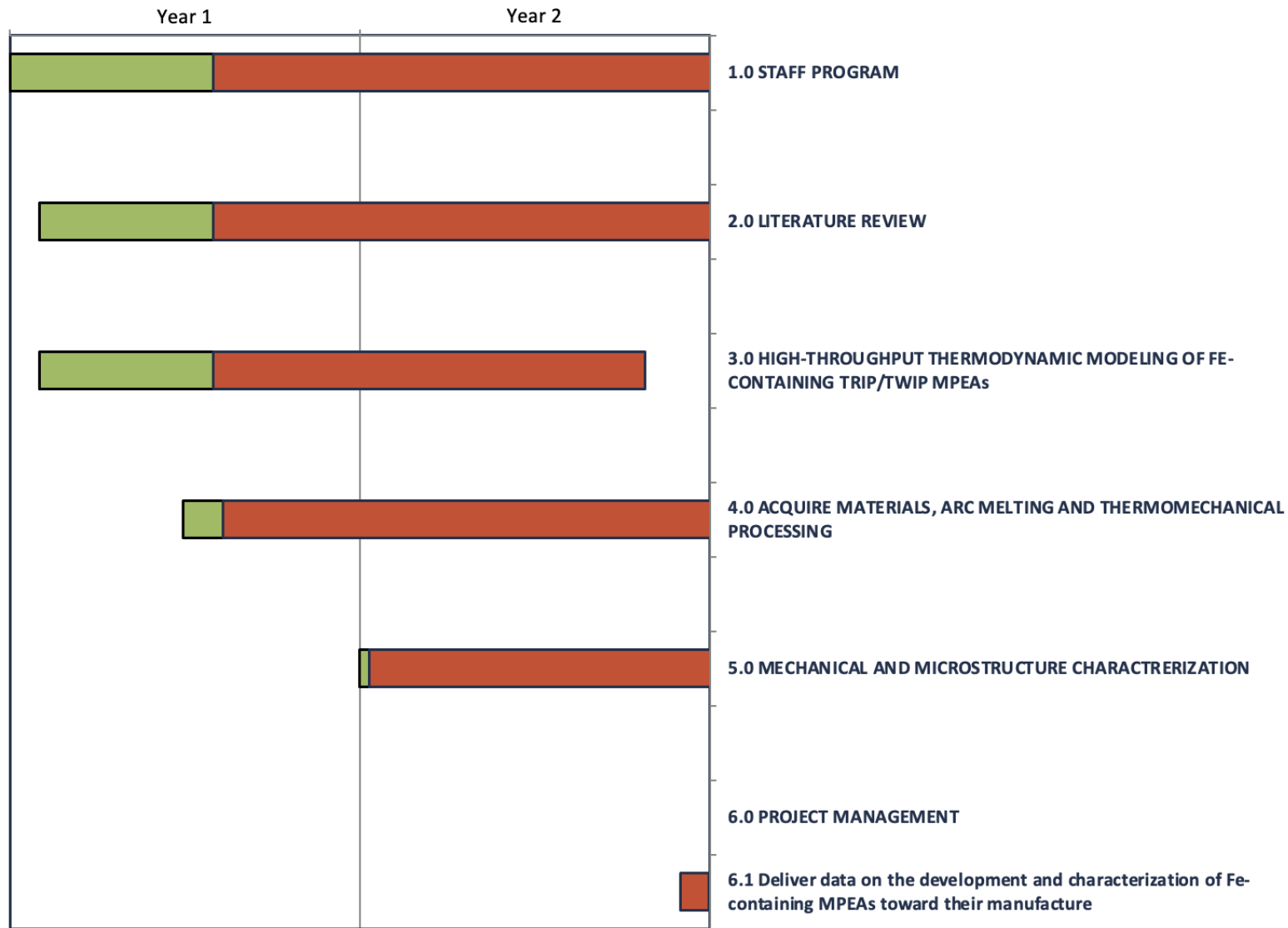
**Datalloy HP**  
 **$T/T_0 = 0.13$  (FCC → BCC)**

# Year 1 Roadmap

- High-throughput thermodynamic modeling
  - ThermoCalc & PanDat –  $T_0$ , precipitation, phase diagrams
  - LAMMPS – SFE, SRO
  - TC-EARS models – solid solution strengthening
- Gleeble thermomechanical processing of baseline commercial products (ATI) – **Materials are on campus**
- Rapid small-scale arc melting of promising Fe-MPEAs – **Equipment ready for commissioning**



# Gantt Chart



# Acknowledgements



- This program is sponsored by the Defense Logistics Agency – Troop Support, Philadelphia PA and the Defense Logistics Agency Information Operations, J68, Research & Development, Ft. Belvoir, VA.
- Special thanks is also given to ATI Specialty Materials for providing test materials.

***Thank you for your time!  
Questions?***

## *Supplementary Slides*

# Modified Olson-Cohen SFE Algorithm

$$\gamma_{SFE} = 2\rho \Delta G^{\gamma \rightarrow \varepsilon} + 2\sigma \quad \rho = \frac{4}{\sqrt{3}} \frac{1}{a^2 N}$$

interstitial nitrogen

$$\Delta G_{N(bulk)}^{\gamma \rightarrow \varepsilon} = E_N^\varepsilon - E_N^\gamma \quad (\text{see Eq. 12})$$

$$\Delta G^{\gamma \rightarrow \varepsilon} = \sum_i \chi_i \Delta G_i^{\gamma \rightarrow \varepsilon} + \sum_{ij} \chi_i \chi_j \Omega_{ij}^{\gamma \rightarrow \varepsilon} + \Delta G_{mg}^{\gamma \rightarrow \varepsilon} + \Delta G_{seg(int)}^{\gamma \rightarrow \varepsilon}$$

substitutionals

$$\Delta G_\phi^{\gamma \rightarrow \varepsilon} = (G_\phi^\varepsilon - G_\phi^\gamma)$$

$$G_\phi^\Phi = a + bT + cT \ln(T) + \sum dT^n$$

$$\Omega_{\phi\phi}^{\gamma \rightarrow \varepsilon} = ({}^0L^\varepsilon - {}^0L^\gamma) + ({}^1L^\varepsilon - {}^1L^\gamma)(\chi_\phi - \chi_\phi)$$

$$\Delta G_{mg}^{\gamma \rightarrow \varepsilon} = G_{mg}^\varepsilon - G_{mg}^\gamma$$

$$G_{mg}^\Phi = RT \ln(\beta^\Phi + 1) f^\Phi(\tau^\Phi)$$

$\tau^\Phi : 1$

$\tau^\Phi > 1$

$$\tau^\Phi = T / T_{N\acute{e}el}^{\Phi}$$

$$f^\Phi(\tau^\Phi) = -\left[ \frac{\tau^{-5}}{10} + \frac{\tau^{-15}}{315} + \frac{\tau^{-25}}{1500} \right] / D$$

$$D = \frac{518}{1125} + \frac{11692}{15975} \left( \frac{1}{p} - 1 \right)$$

$$f^\Phi(\tau^\Phi) = 1 - \left[ \frac{79\tau^{-1}}{140p} + \frac{474}{497} \left( \frac{1}{p} - 1 \right) \left( \frac{\tau^3}{6} + \frac{\tau^9}{135} + \frac{\tau^{15}}{600} \right) \right] / D$$

$a$ : lattice parameter  
 $a, b, c, d$ : coefficients  
 $G_\phi^\Phi$ : Gibbs energy of pure elements  
 $G_{mg}^\Phi$ : magnetic contribution to Gibbs energy  
 ${}^0L^p$ : linear function of  $T$   
 ${}^1L^p$ : constant  
 $n$ : set of integers  
 $N$ : Avogadro's constant  
 $p$ : fraction of magnetic enthalpy absorbed above  $T_{N\acute{e}el}$   
 $R$ : gas constant  
 $T_{N\acute{e}el}, T$ : (Néel) temperature

$V$ : molar volume  
 $\beta^\Phi$ : magnetic moment  
 $\Delta G^{\gamma \rightarrow \varepsilon}, \Delta G_\phi^{\gamma \rightarrow \varepsilon}, \Delta G_{mg}^{\gamma \rightarrow \varepsilon}$   
 $\Delta G_{seg(int)}^{\gamma \rightarrow \varepsilon}$  ( $\Delta G_{chem(int)}^{\gamma \rightarrow \varepsilon}, \Delta G_{surf(int)}^{\gamma \rightarrow \varepsilon}$ )  
 $\Delta G_{el(int)}^{\gamma \rightarrow \varepsilon}$ : change in Gibbs energy upon  $\gamma - \varepsilon$  phase transformation, chemical, magnetic, and nitrogen segregation contributions (chemical, surface, elastic)

$\gamma_{SFE}$ : stacking fault energy  
 $\mu$ : shear modulus  
 $\Omega_{\phi\phi}^{\gamma \rightarrow \varepsilon}$ : excess free energies  
 $\Lambda$ : nitrogen atom-dislocation interaction energy  
 $\rho$ :  $\{111\}$  molar surface density  
 $\sigma$ :  $\gamma/\varepsilon$ -interface energy  
 $\nu$ : Poisson's ration  
 $\chi$ : molar fractions

$$\Delta G_{chem(int)}^{\gamma \rightarrow \varepsilon} = RT \left[ \chi_{N(bulk)} \ln \frac{\chi_{N(seg)}}{\chi_{N(bulk)}} + (1 - \chi_{N(bulk)}) \ln \frac{1 - \chi_{N(seg)}}{1 - \chi_{N(bulk)}} \right]$$

$$\Delta G_{seg(int)}^{\gamma \rightarrow \varepsilon} = \Delta G_{chem(int)}^{\gamma \rightarrow \varepsilon} + \Delta G_{surf(int)}^{\gamma \rightarrow \varepsilon} + \Delta G_{el(int)}^{\gamma \rightarrow \varepsilon}$$

$$\Delta G_{surf(int)}^{\gamma \rightarrow \varepsilon} = \frac{1}{4} \Lambda (\chi_{N(seg)} - \chi_{n(bulk)})^2$$

$$\Delta G_{el(int)}^{\gamma \rightarrow \varepsilon} = \frac{2}{9} \mu \frac{1+\nu}{1-\nu} \left( \frac{dV}{dX} \right) \frac{1}{V} (\chi_{N(seg)} - \chi_{N(bulk)})$$

Curtze, S., V. T. Kuokkala, A. Oikari, J. Talonen, and H. Hänninen. "Thermodynamic Modeling of the Stacking Fault Energy of Austenitic Steels." *Acta Materialia* 59, no. 3 (February 1, 2011): 1068–76. <https://doi.org/10.1016/J.ACTAMAT.2010.10.037>.



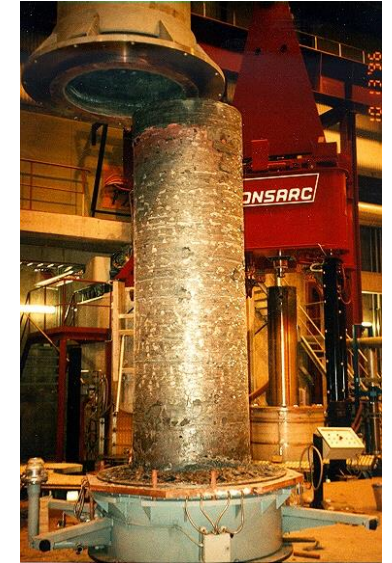
# Industry Partner – ATI Specialty Materials

## Added Capability

- 25 & 50 lb. vacuum melted ingots
- VAR/ESR for cleanliness
- Industrial thermomechanical processing & heat treatment

## Baseline Alloys

- ATI 188 – Co-base high-temp austenitic alloy; high work-hardening; TRIP?
- A286 – Legacy NiCr high-temp austenitic steel; TRIP?
- Datalloy HP – Highly alloyed steel; quasi-MPEA



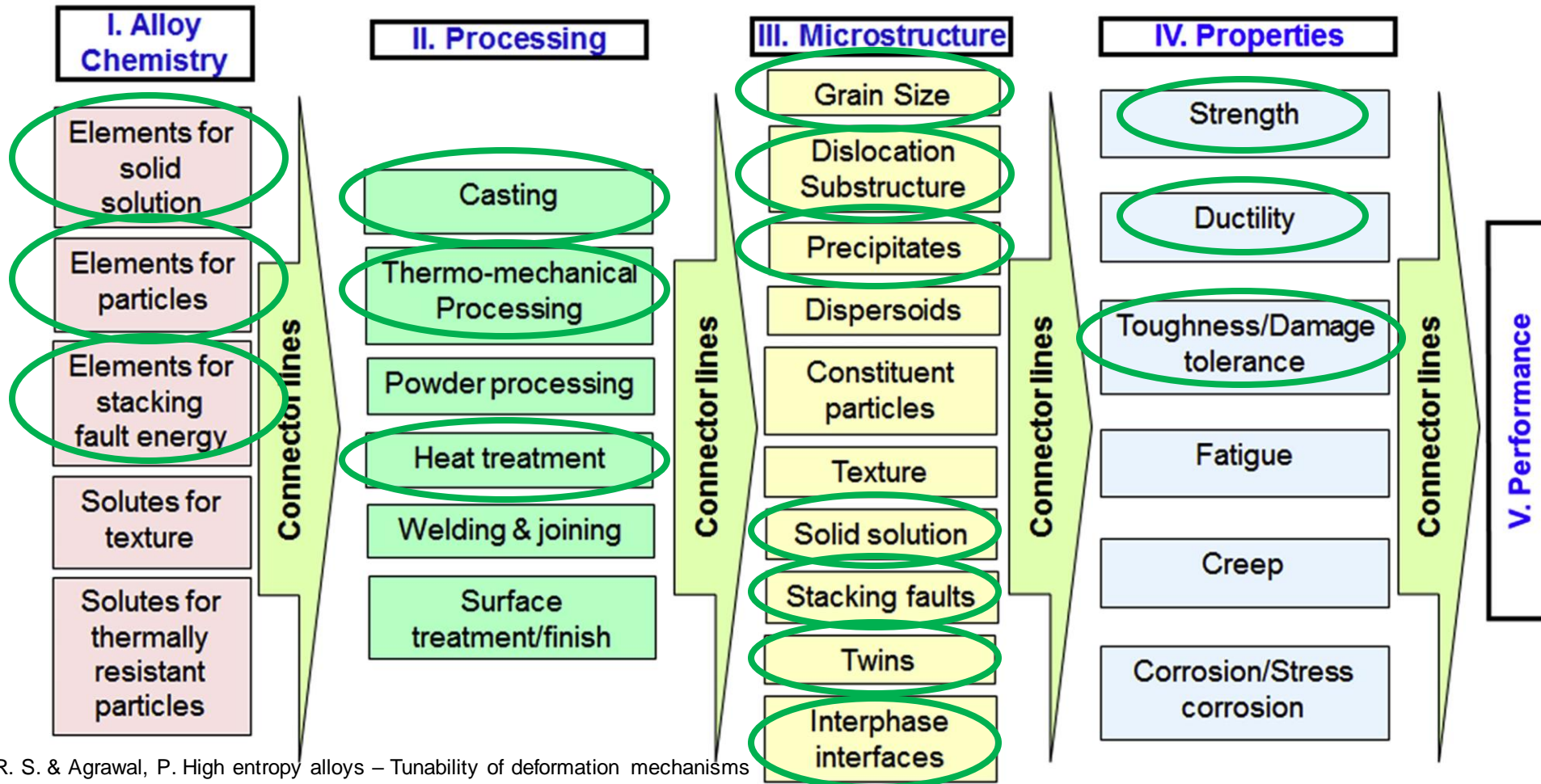
Composition Range (UNS N08830)			
Element	Wt. %	Element	Wt. %
Carbon	0.015	Manganese	3.0 – 6.0
Phosphorous	0.035	Sulfur	0.010
Silicon	1.00	Nickel	29.0 – 34.0
Chromium	20.0 – 24.0	Molybdenum	4.5 – 6.5
Copper	0.50 – 2.00	Cobalt	0.50 – 3.50
Tungsten	0.20 – 1.80	Nitrogen	0.20 – 0.55
Iron	balance		

Maximum % unless a range is indicated.

**Datalloy HP**  
 **$T/T_0 = 0.13$  (FCC → BCC)**

# Performance-Driven Systems Approach to Alloy Design

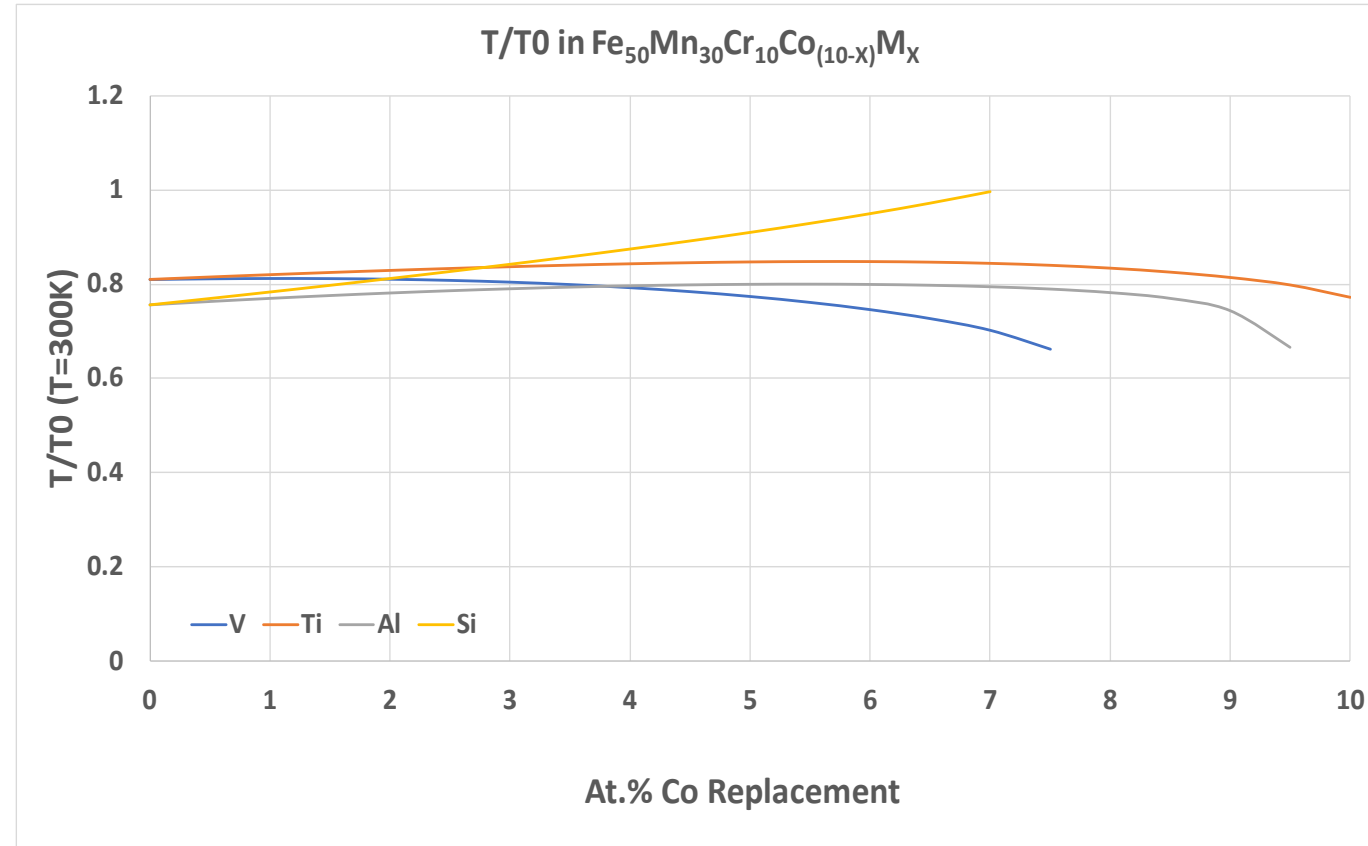
Modified Olson's Materials Systems Approach Chart for Alloy Design



Mishra, R. S., Haridas, R. S. & Agrawal, P. High entropy alloys – Tunability of deformation mechanisms through integration of compositional and microstructural domains. *Materials Science and Engineering A* vol. 812 141085 (2021).

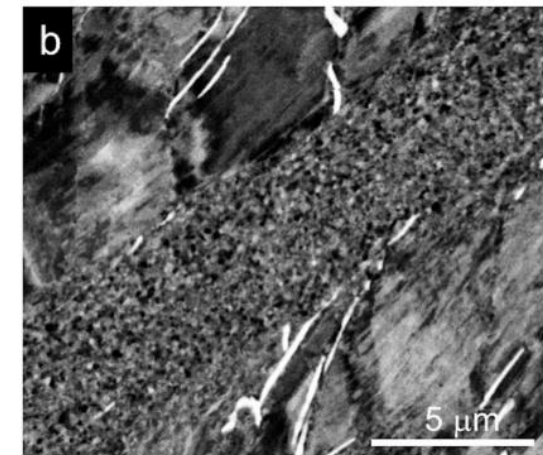
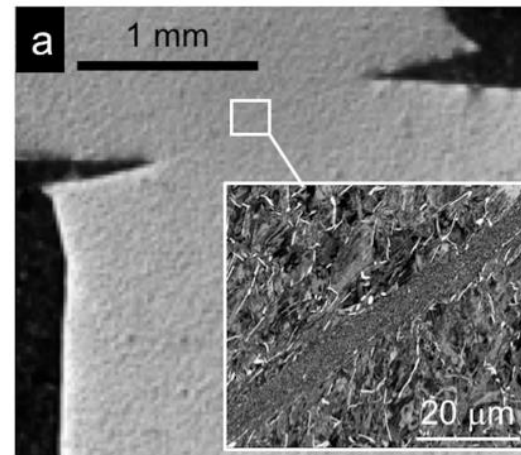
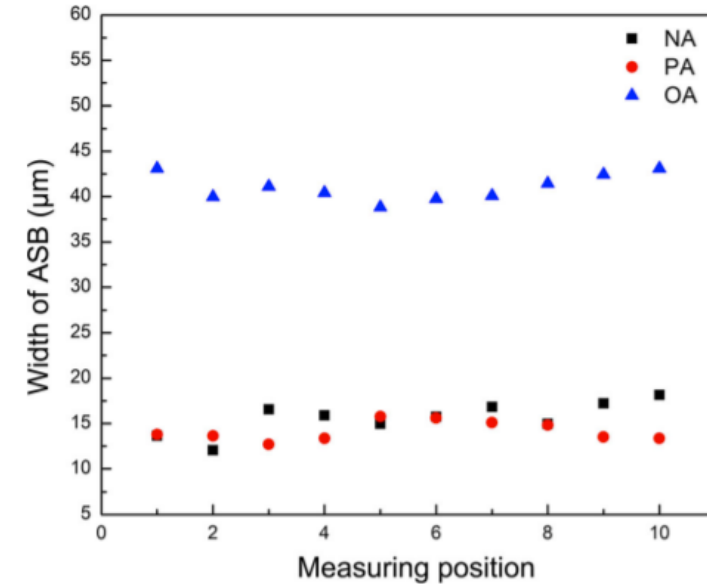
# $T_0$ Screening - $\text{Fe}_{50}\text{Mn}_{30}\text{Cr}_{10}\text{Co}_{(10-x)}\text{M}_x$ Family

- Tried many  $\text{Fe}_{50}\text{Mn}_{30}\text{Cr}_{10}\text{Co}_{(10-x)}\text{M}_x$  derivatives of landmark TRIP-MPEA
- V, Ti, Al all reduce  $T/T_0$  (i.e promote TRIP)
- V is strongest  $T/T_0$  reducer
- Problem – avoiding  $\sigma$  phase formation – need kinetics studies
- Are  $\text{M}_{23}\text{C}_6$ ,  $\text{M}_7\text{C}_3$  &  $\eta$  carbides preferable to  $\sigma$  in this setting?

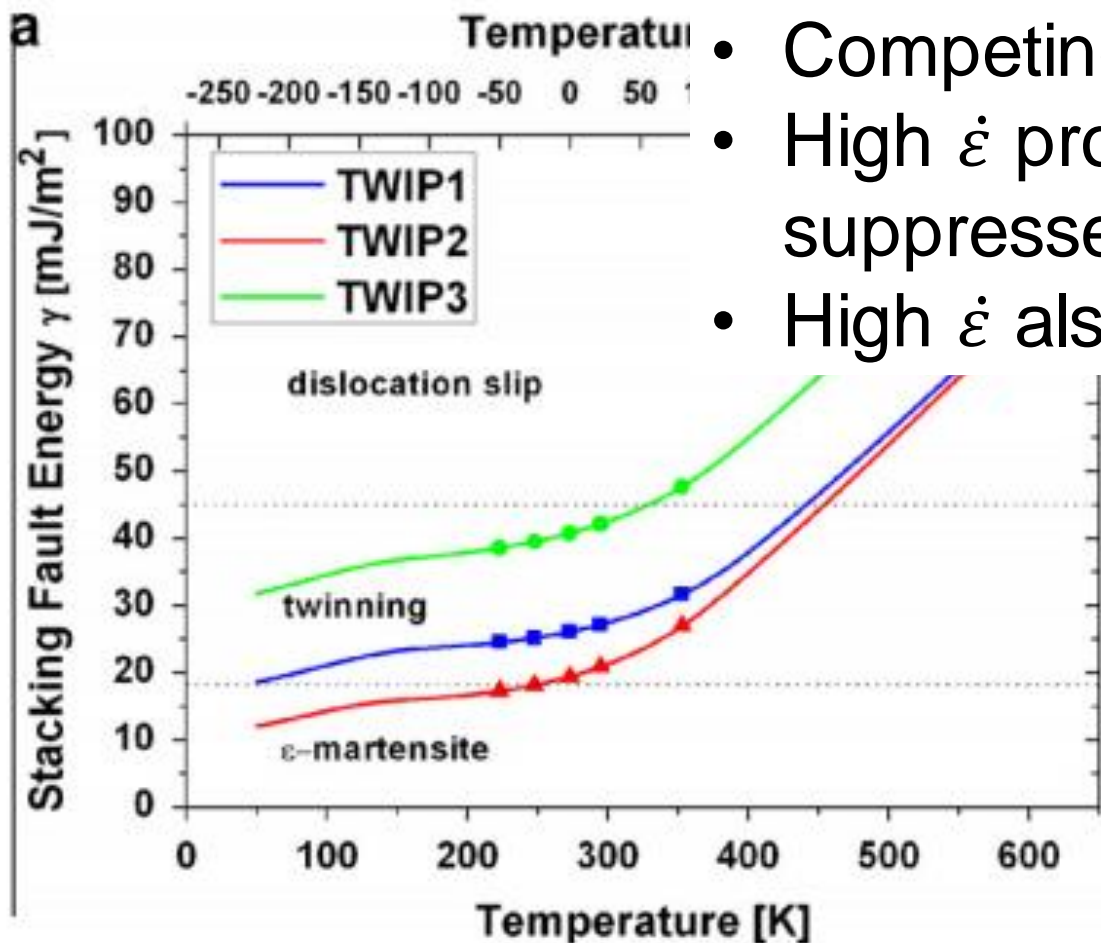


# Adiabatic Shear Banding & Microstructure

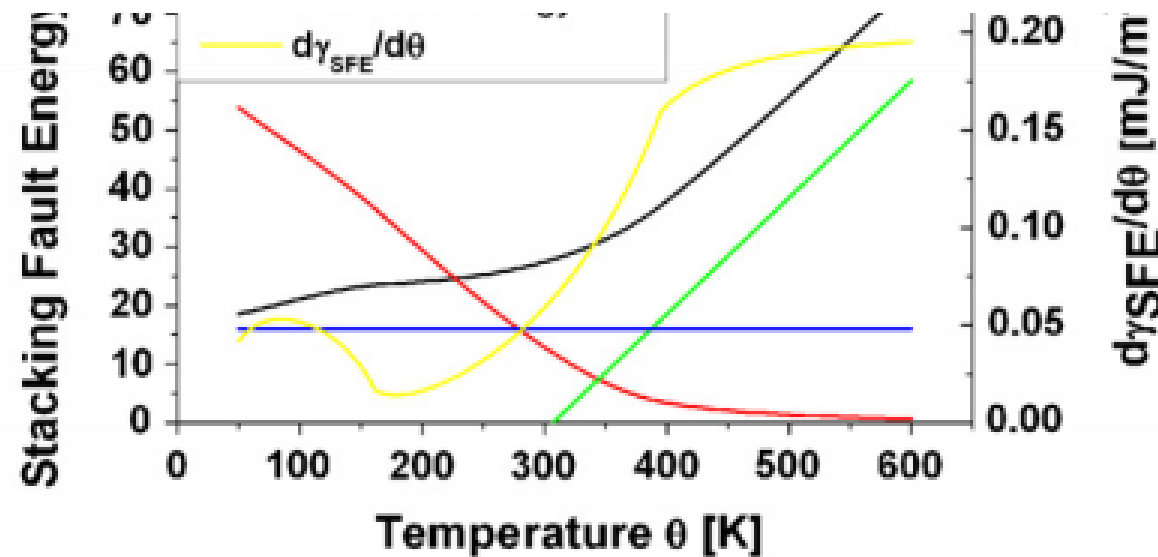
- Some evidence that aging affects ASB formation, morphology
- Zhang et al. (*J Mater Sci* June 2020) – ASBs in Al-Zn-Mg-Cu wider in overaged vs peak
- Wider ASB → higher critical strain/strain rate to form (Xue et al., *Acta* 44 1996)
- Peak age vs overage – different substructure in dynamic loading → diff shear localization behavior
- Torsion Kolsky best way to assess
- Also evidence of ASB dissolution of  $\gamma'$  (Colliander et al. *Phil Letters* Sept 2020)



# SFE, Temperature & Strain Rate Effects on Deformation Mechanism



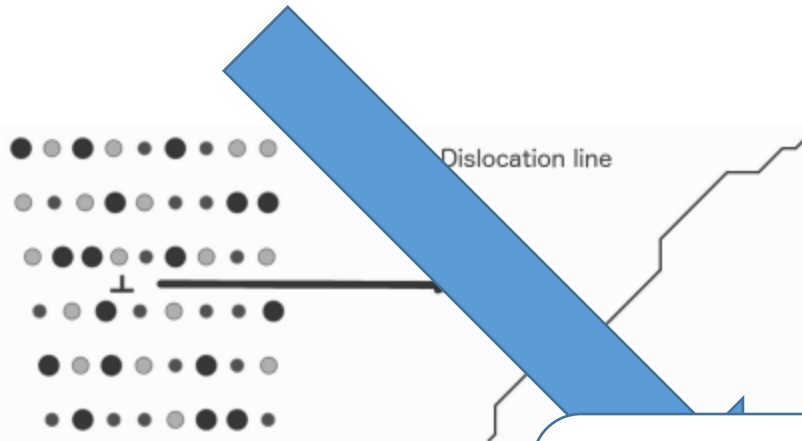
- Competing  $\dot{\epsilon}$  effects
- High  $\dot{\epsilon}$  promotes twinning, but also raises  $T \rightarrow$  suppresses twinning
- High  $\dot{\epsilon}$  also promotes HCP TRIP but not BCC



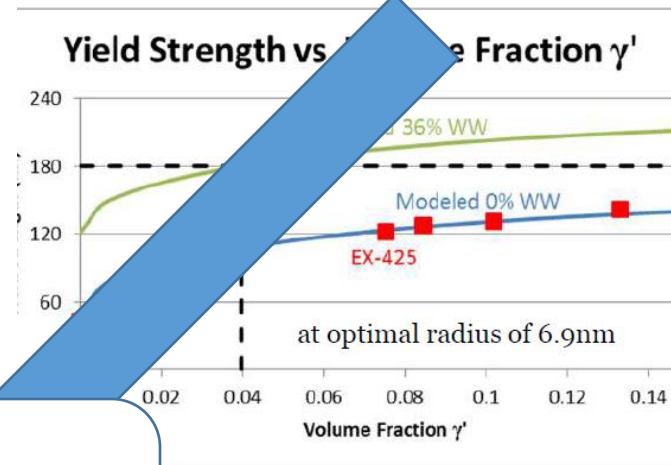
Curtze, S., and V. T. Kuokkala. "Dependence of Tensile Deformation Behavior of TWIP Steels on Stacking Fault Energy, Temperature and Strain Rate." *Acta Materialia* 58, no. 15 (September 1, 2010): 5129–41. <https://doi.org/10.1016/J.ACTAMAT.2010.05.049>.

# Alloy Design Strategy – Yield Strength

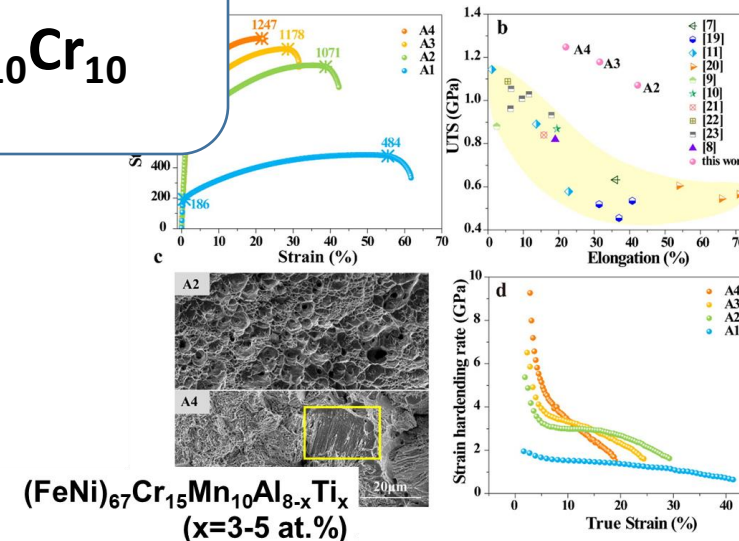
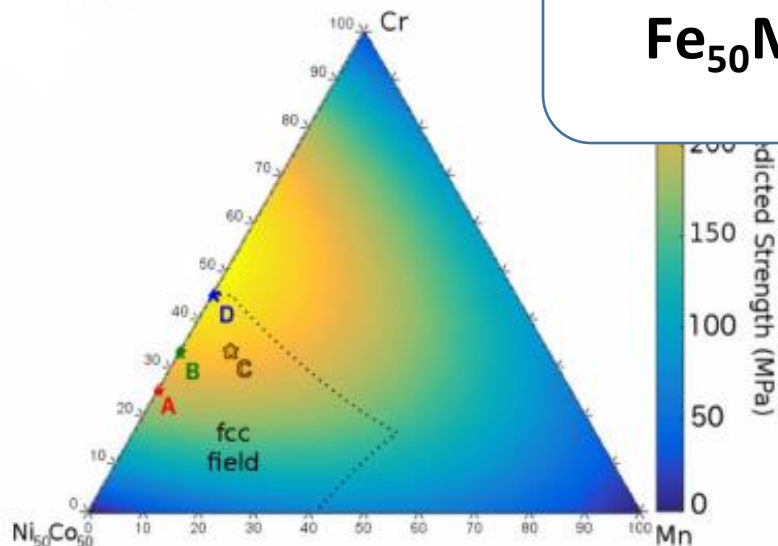
## Solid Solution Strengthening



## $\gamma'$ Precipitate Strengthening

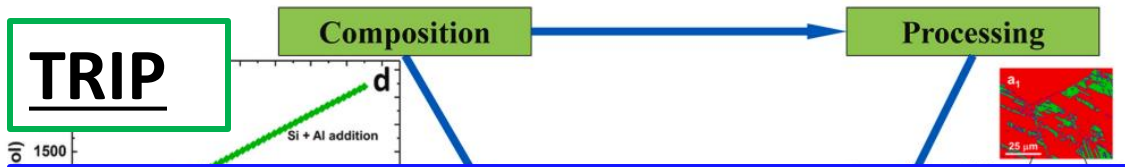


Improved YS over  $\text{Fe}_{50}\text{Mn}_{30}\text{Co}_{10}\text{Cr}_{10}$

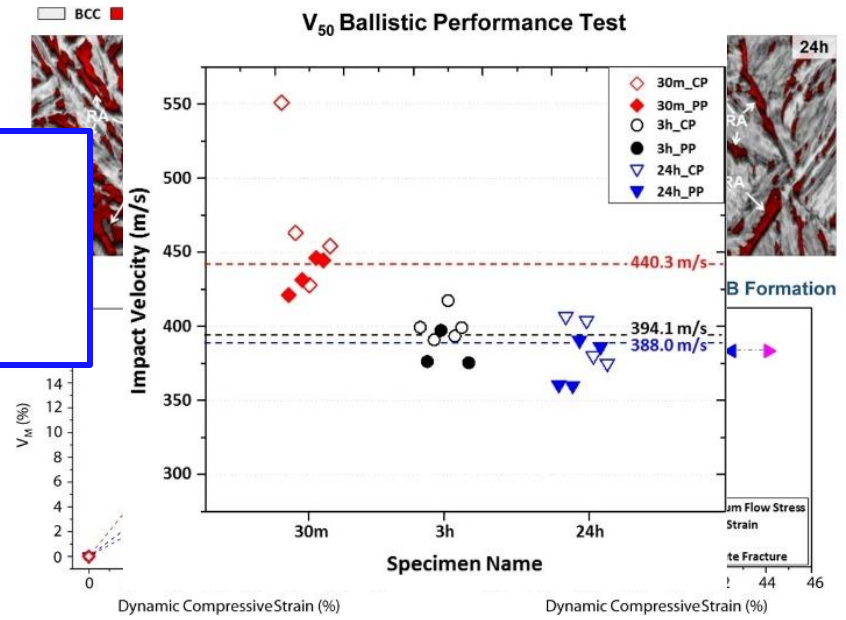
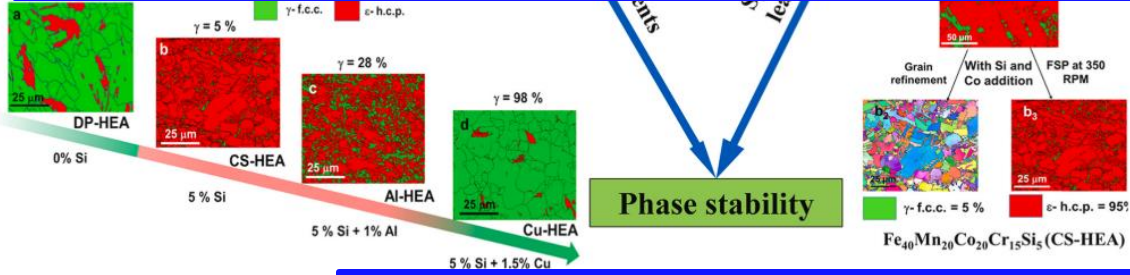


Zhao, Y. L. et al. Development of high-strength Co-free high-entropy alloys hardened by nanosized precipitates. *Scr. Mater.* 148, 51–55 (2018).

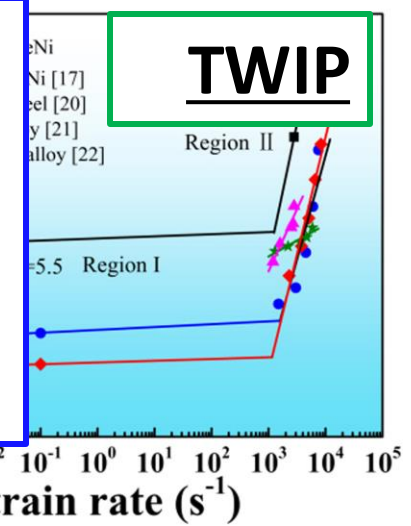
# Alloy Design Strategy – Post-Yield Behavior



- V&V'd modeling approach ( $T_0$ ) for TRIP
- Computationally cheap
- Database-sensitive, not yet mature in MPEAs



- TWIP considered to have attractive ballistic properties
- TWIP harder to predict (stacking fault energy)
- SFE good predictor for both TWIP & TRIP
- Computationally expensive, more expertise required (DFT)
- Thermodynamic methods (Olson-Cohen) not fully validated for MPEAs



W. Jiang et al, Dynamic impact behavior and deformation mechanisms of Cr26Mn20Fe20Co20Ni14 high-entropy alloy, *Mater Sci Eng A* (824) September 2021

L. Wang et al, Mechanical response and deformation behavior of Al0.6CoCrFeNi high-entropy alloys upon dynamic loading, *Mater Sci Eng A* (727) June 2018

# End User Context – Growth in Protective Structure Requirements

